Acta Crystallographica Section F
Structural Biology and Crystallization Communications
ISSN 1744-3091

Crystallization and preliminary X-ray diffraction analysis of the azoreductase PpAzoR from *Pseudomonas putida* MET94

Bruno Correia,‡ Zhenjia Chen,‡ Sónia Mendes, Lígia O. Martins and Isabel Bento*

Instituto de Tecnologia Química e Biológica, Universidade Nova de Lisboa, Avenida da República, 2780-257 Oeiras, Portugal

‡ These authors contributed equally to this work.

Correspondence e-mail: bento@itqb.unl.pt

Received 3 September 2010
Accepted 18 November 2010

PpAzoR, an FMN-dependent NADPH azoreductase from *Pseudomonas putida* MET94, has been crystallized using the sitting-drop vapour-diffusion technique. The crystals diffracted to 1.6 Å resolution using synchrotron radiation and belonged to the orthorhombic space group *F*222, with unit-cell parameters $a = 72.1$, $b = 95.5$, $c = 146.1$ Å. Data sets were collected from the native protein to 2.2 Å resolution using in-house equipment and to 1.6 Å resolution using synchrotron radiation and the three-dimensional structure was determined by the molecular-replacement method.

1. Introduction

Azo dyes are synthetic compounds that contain one or more azo bonds (—N═N—). These dyes are extensively used in the textile, cosmetics, printing and food-colouring industries owing to their chemical stability and ease of synthesis (Meyer, 1981). However, their strong stability constitutes a problem for the environment as these dyes are usually found in a chemically unchanged pollutant form even after wastewater treatment (Holme *et al.*, 1984). Nevertheless, despite their potentially toxic and carcinogenic properties (Alves de Lima *et al.*, 2007) there are more than 2000 azo dyes and they make up around 50% of world dye production (Stolz, 2001; Alves de Lima *et al.*, 2007). This fact has led to a demand for more efficient technologies for the degradation of azo dyes. Degradation treatments based on chemical procedures are expensive, require a lot of energy and often yield hazardous byproducts. In contrast, biological degradation of azo dyes performed by microorganisms can be undertaken under mild conditions, avoiding these problems. Indeed, a variety of microorganisms have been shown to be able to decolourize a diverse range of azo dyes (Levine, 1991). The dye-degrading enzymes that have been characterized to date are able to catalyze the reduction of azo dyes in the presence of NAD(P)H, transforming a number of them into colourless aromatic amines by cleaving the azo groups (Chen, 2006). These enzymes are azobenzene reductases, commonly known as azoreductases, and contain a flavin mononucleotide (FMN or FAD) as a prosthetic group (Mueller & Miller, 1949). Azoreductases have also been a subject of interest for the pharmaceutical industry. These enzymes, which are also expressed by the gastrointestinal microflora, have the ability to activate anti-inflammatory azo prodrugs such as 5-aminosalicylate-based compounds that are used to treat inflammatory bowel diseases (Peppercorn & Goldman, 1972). These enzymes have been shown to reduce azo compounds *via* a ping-pong bi-bi mechanism that requires two cycles of NADPH-dependent reduction of FMN to $FMNH_2$ (Ryan *et al.*, 2010, and references therein). In the first cycle the azo substrate is reduced to a hydrazine and in the second cycle the hydrazine is concomitantly reduced to two amines. Enzymes with azoreductase activity have been confirmed in many bacterial species and several crystallographic studies of enzymes from different origins have already been reported (Ito *et al.*, 2006, 2008; Wang *et al.*, 2007, 2010; Binter *et al.*, 2009; Ryan

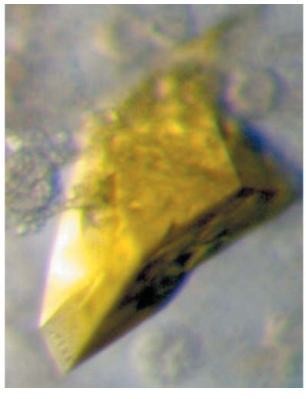

Table 1
Data-collection statistics.

	X8 PROTEUM diffractometer	Beamline ID14-4 at ESRF
Wavelength (Å)	1.54	0.95
Detector	CCD area detector	ADSC Quantum Q315r
Crystal-to-detector distance (mm)	65.0	226.1
Resolution (Å)	2.2 (2.30–2.20)	1.6 (1.65–1.60)
Scan type	ω scan	φ scan
Oscillation angle (°)	0.5	0.75
Total angular range (°)	671†	113.25
Exposure time per image (s)	60	1
Space group	*F*222	*F*222
Unit-cell parameters (Å)	a = 72.1, b = 95.5, c = 146.1	a = 72.3, b = 95.7, c = 146.5
Mosaicity (°)	0.98	0.80
Total No. of observations	165332	143284
No. of unique reflections	12976 (1596)	33249 (4846)
Completeness (%)	99.7 (100.0)	99.1 (100.0)
Multiplicity	10.5 (7.3)	4.3 (4.4)
Mean $I/\sigma(I)$	18.8 (3.5)	13.9 (3.6)
R_{merge} (%)	5.6 (29.0)	5.1 (32.1)
Overall B factor from Wilson plot (Å^2)	27.3	19.7

† In eight different crystal settings.

et al., 2010); however, their physiological role remains unclear (Ryan *et al.*, 2010). With the aim of engineering an enzyme for biotechnological applications and to contribute to understanding the catalytic process that underlies the biodegradation of recalcitrant azo dyes, we have determined the three-dimensional structure of the FMN-dependent NADPH azoreductase (PpAzoR) from *Pseudomonas putida* MET94, which was selected as a highly versatile bacterium for dye decolourization (Mendes *et al.*, 2011). In this study, we report the crystallization and preliminary X-ray diffraction analyses of PpAzoR crystals.

2. Experimental procedures

2.1. Cloning, expression and purification

The *ppAzoR* gene (accession No. NP_745010), which encodes a 203 amino-acid residue protein, was cloned into the expression vector pET-21a(+) (Novagen) and heterologously produced in *Escherichia coli* Tuner (DE3) (Novagen). The recombinant protein was purified in three chromatographic steps: briefly, a Q-Sepharose column followed by a Mono-Q 5/50 column (GE Healthcare Biosciences) and a Superdex 200 HR 10/30 column (GE Healthcare Biosciences) equilibrated with 20 m*M* Tris–HCl buffer pH 7.6 containing 0.2 *M* NaCl (Mendes *et al.*, 2011). Active fractions were pooled, concentrated and stored at 253 K until use. SDS–PAGE analysis revealed a molecular mass of ∼23 kDa (Fig. 1), whereas size-exclusion chromatography yielded a native molecular mass of approximately 40 kDa, demonstrating that the recombinant PpAzoR1 forms a homodimer in solution, similar to previous observations for other flavin-dependent azoreductases (Chen *et al.*, 2004; Ito *et al.*, 2006; Liu *et al.*, 2007; Nakanishi *et al.*, 2001).

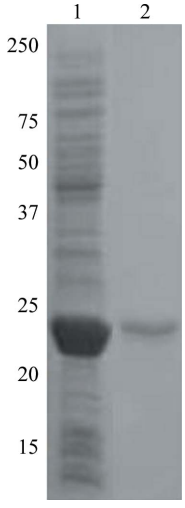

Figure 1
SDS–PAGE analysis of purified recombinant PpAzoR. Lane 1, crude extract of recombinant *E. coli* cells overproducing PpAzoR; lane 2, purified enzyme.

2.2. Crystallization

Crystallization screens were prepared in 96-well plates using the sitting-drop vapour-diffusion technique with a Cartesian robot. Each drop, consisting of 100 nl protein solution and 100 nl reservoir solution, was equilibrated against reservoir solution at 293 K. Once crystalline material had been identified (solution G1 from the NeXtal Classics Suite), a scale-up of the process was undertaken in 48-well plates with 3 µl drops (1.5 µl protein solution plus 1.5 µl reservoir solution) in order to obtain well diffracting crystals. PpAzoR crystals (Fig. 2) suitable for data collection were obtained after ∼10 d using protein solution at a concentration of 28 mg ml^{-1} (as measured by the Bradford assay with bovine serum albumin as standard) containing 2 m*M* FMN and reservoir solution consisting of 4% PEG 400, 2 *M* ammonium sulfate and 0.1 *M* HEPES pH 7.0 at 293 K.

2.3. X-ray analysis and structure solution

Crystals were cryoprotected with paraffin oil and flash-cooled under liquid nitrogen and initial crystal characterization was undertaken using in-house equipment (X8 PROTEUM diffractometer) at 110 K. The crystals diffracted to 2.2 Å resolution (the data statistics are listed in Table 1) and belonged to the orthorhombic space group *F*222, with unit-cell parameters a = 72.1, b = 95.5, c = 146.1 Å. The crystals contained one molecule per asymmetric unit, corresponding to a Matthews coefficient of 2.78 Å^3 Da^{-1} and a solvent content of 56% (Matthews, 1968). This data set was processed and scaled with the programs *SAINT* and *SADABS*, respectively, as part of the

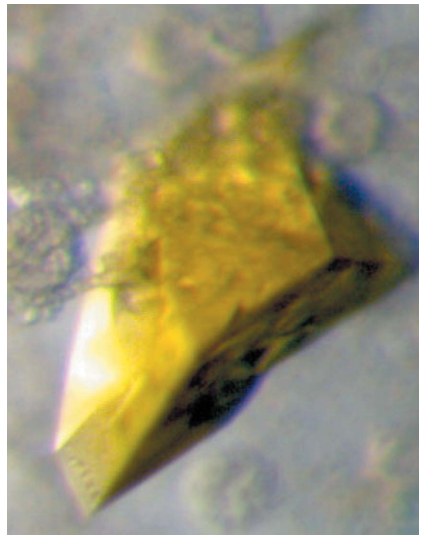

Figure 2
A crystal of PpAzoR obtained from a reservoir solution consisting of 4% PEG 400, 2 *M* ammonium sulfate and 0.1 *M* HEPES pH 7.0 at 293 K with average dimensions of 0.2 × 0.1 × 0.05 mm.

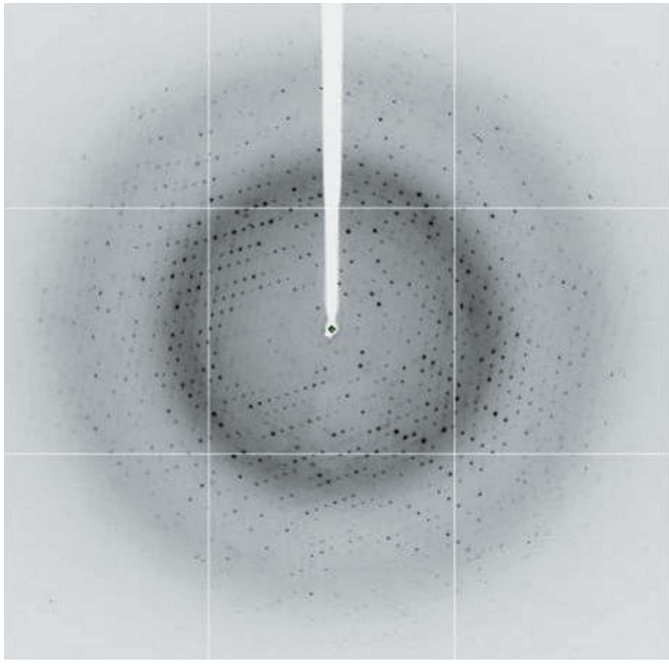

Figure 3
Diffraction image of a PpAzoR crystal collected on beamline ID14-4 at ESRF in Grenoble.

Bruker AXS *PROTEUM* software suite and the data statistics were obtained with *XPREP* (Bruker AXS). The three-dimensional structure of PpAzoR was solved by molecular replacement with the program *MOLREP* (Vagin & Teplyakov, 2010), using the azoreductase from *E. coli* (PDB code 2z9d; Ito *et al.*, 2008), which shows 46% sequence identity, as a search model. The correct solution given by the program *MOLREP* showed a score of 71.7% and an *R* factor of 43.7%, whereas the first noise solution showed a score and an *R* factor of 36.1% and 63.1%, respectively. A second data set (Fig. 3) with higher resolution was then obtained on beamline ID14-4 at ESRF, Grenoble. These data were processed and scaled with the programs *MOSFLM* (Leslie, 2006) and *SCALA* (Evans, 2006) (the data-collection statistics are listed in Table 1) and are being used to refine the three-dimensional structure of PpAzoR.

Maria Arménia Carrondo is gratefully acknowledged for support. The provision of synchrotron-radiation facilities and the assistance of the macromolecular crystallography staff at the European Synchrotron Radiation Facility, Grenoble, France are sincerely acknowledged.

References

Alves de Lima, R. O., Bazo, A. P., Salvadori, D. M., Rech, C. M., de Palma Oliveira, D. & de Aragao Umbuzeiro, G. (2007). *Mutat. Res.* **626**, 53–60.
Binter, A., Staunig, N., Jelesarov, I., Lohner, K., Palfey, B. A., Deller, S., Gruber, K. & Macheroux, P. (2009). *FEBS J.* **276**, 5263–5274.
Chen, H. (2006). *Curr. Protein Pept. Sci.* **7**, 101–111.
Chen, H., Wang, R.-F. & Cerniglia, C. E. (2004). *Protein Expr. Purif.* **34**, 302–310.
Evans, P. (2006). *Acta Cryst.* D**62**, 72–82.
Holme, I., Helgeland, A., Hjermann, I., Leren, P. & Lund-Larsen, P. G. (1984). *JAMA*, **251**, 1298–1299.
Ito, K., Nakanishi, M., Lee, W.-C., Sasaki, H., Zenno, S., Saigo, K., Kitade, Y. & Tanokura, M. (2006). *J. Biol. Chem.* **281**, 20567–20576.
Ito, K., Nakanishi, M., Lee, W.-C., Zhi, Y., Sasaki, H., Zenno, S., Saigo, K., Kitade, Y. & Tanokura, M. (2008). *J. Biol. Chem.* **283**, 13889–13896.
Leslie, A. G. W. (2006). *Acta Cryst.* D**62**, 48–57.
Levine, W. G. (1991). *Drug. Metab. Rev.* **23**, 253–309.
Liu, G., Zhou, J., Lv, H., Xiang, X., Wang, J., Zhou, M. & Qv, Y. (2007). *Appl. Microbiol. Biotechnol.* **76**, 1271–1279.
Matthews, B. W. (1968). *J. Mol. Biol.* **33**, 491–497.
Mendes, S., Pereira, L. Batista, C. & Martins, L. O. (2011). Submitted.
Meyer, U. (1981). *FEMS Symp.* **12**, 371–385.
Mueller, G. C. & Miller, J. A. (1949). *J. Biol. Chem.* **180**, 1125–1136.
Nakanishi, M., Yatome, C., Ishida, N. & Kitade, Y. (2001). *J. Biol. Chem.* **276**, 46394–46399.
Peppercorn, M. A. & Goldman, P. (1972). *J. Pharmacol. Exp. Ther.* **181**, 555–562.
Ryan, A., Laurieri, N., Westwood, I., Wang, C.-J., Lowe, E. & Sim, E. (2010). *J. Mol. Biol.* **400**, 24–37.
Stolz, A. (2001). *Appl. Microbiol. Biotechnol.* **56**, 69–80.
Vagin, A. & Teplyakov, A. (2010). *Acta Cryst.* D**66**, 22–25.
Wang, C.-J., Hagemeier, C., Rahman, N., Lowe, E., Noble, M., Coughtrie, M., Sim, E. & Westwood, I. (2007). *J. Mol. Biol.* **373**, 1213–1228.
Wang, C.-J., Laurieri, N., Abuhammad, A., Lowe, E., Westwood, I., Ryan, A. & Sim, E. (2010). *Acta Cryst.* F**66**, 2–7.